Recent Results of GRB X-ray Afterglows

David N. Burrows[1]

[1] Dept. of Astronomy & Astrophysics, The Pennsylvania State University,
525 Davey Lab, University Park, PA 16802, USA
E-mail(DNB): burrows@astro.psu.edu

ABSTRACT

I review recent results on GRB X-ray afterglows measured by the *Swift* X-ray Telescope (XRT). The XRT had observed over 290 X-ray afterglows of GRBs at the time of this meeting, obtaining $> 80\%$ of the world total of GRB X-ray afterglows and $> 70\%$ of the world total of GRBs with redshifts. I discuss general characteristics of X-ray afterglows as observed by *Swift*, and will then focus on a few of our most interesting discoveries. One of the most exciting of these was the recent "naked-eye" burst, GRB 080319B, with the brightest optical counterpart ever seen and one of the best-observed X-ray and optical light curves ever obtained. We interpret the bright prompt emission as the result of an extremely large bulk Lorentz factor, combined with a very narrow jet beamed directly at us, with Synchrotron Self-Compton emission from the UV/optical photons accounting for the γ-ray emission. The X-ray and optical afterglows are interpreted as the result of a two-component jet, with the wide jet accounting for the optical afterglow, while the X-ray afterglow is initially dominated by the narrow jet until that component fades following its jet break.

KEY WORDS: missions: Swift — GRBs: X-ray afterglows — GRB 080319B

1. Introduction

In the first 30 years since the discovery of Gamma-ray Bursts (GRBs) in 1967 (Klebesadel et al. 1973), GRBs had been found to have an isotropic distribution on the sky and a volume-limited distribution in distance (Meegan et al. 1992). It was also known that the distribution of GRB durations (typically defined as t_{90}, the time during which 90% of the fluence was detected) was bimodal (Fig. 1), with one peak at subsecond durations (generally referred to as "short" GRBs) and another peak at tens of seconds ("long" GRBs) (Kouveliotou et al. 1993). Little was known about the progenitors and hosts of GRBs, and there was debate about whether they represented a local population of objects or were distributed at cosmological distances. This debate was resolved in 1997 with the Beppo-SAX discoveries of the first GRB afterglows, their localization to arcminute accuracy, and the subsequent identification of associated optical transients (Costa et al. 1997; van Paradijs et al. 1997). Redshift measurements determined that GRBs were at cosmological distances (Metzger et al. 1997; Djorgovski et al. 1998). Subsequent associations of a few long GRBs with supernovae, together with the association of long GRBs with star forming regions of their host galaxies (Fruchter et al. 2006), provided evidence that long GRBs are produced during the collapse of massive stars and are probably associated with the formation of black holes. Although not
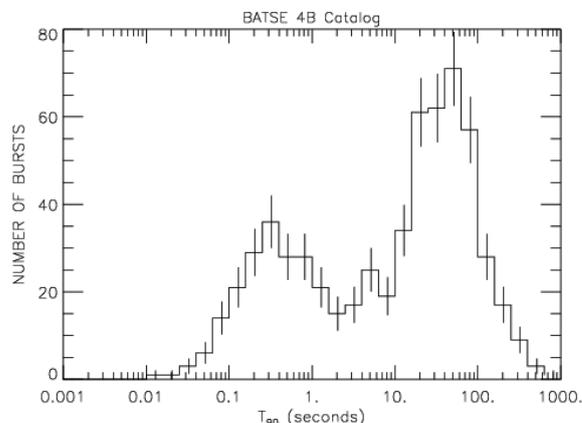

Fig. 1. Distribution of GRB durations measured by the BATSE instrument on the *Compton Gamma-Ray Observatory* (from *http://www.batse.msfc.nasa.gov/batse/grb/duration/*).

localized to similar precision, short GRBs were thought to be associated with mergers of compact objects (Lattimer & Schramm 1976; Paczyński 1986; Eichler et al. 1989; Paczyński 1991).

Observations of GRB afterglows in the optical and X-ray bands agreed well with the predictions of what has become the standard fireball model (Rees & Mészáros

1992; Mészáros & Rees 1993), in which a central engine releases an enormous amount of energy, producing a highly relativistic outflow in the form of a collimated jet. Internal shocks within this outflow are responsible for the prompt gamma-ray emission, while external shocks produced when the outflow encounters the surrounding medium produce a long-lived broadband afterglow.

The launch of the *Swift* satellite (Gehrels et al. 2004) on 20 November 2004 introduced a new era in GRB studies. Whereas *Beppo-SAX* typically required 6-8 hours to begin observing a GRB afterglow (de Pasquale et al. 2006), *Swift* is a highly autonomous robotic observatory, capable of automatically modifying its on-board observing program to incorporate observations of new GRBs and of slewing promptly to them, beginning observations of afterglows within 1-2 minutes after the burst in most cases. It carries 3 instruments: the Burst Alert Telescope (BAT, Barthelmy et al. 2005a), a coded aperture instrument with a 2 sr field of view (FOV) covering the energy band 15-350 keV; the X-ray Telescope (XRT, Burrows et al. 2005), an automated instrument covering the energy range 0.2-10 keV and capable of measuring positions accurate to about 2 arcseconds (Goad et al. 2007, Evans et al. 2008); and the UV/optical telescope (UVOT, Roming et al. 2005) covering the band 170-650 nm with subarcsecond position accuracy. GRB positions are determined on-board to arcminute and often to several arcsecond accuracy and distributed immediately to the Gamma-ray burst Coordinations Network. Subsequent ground processing generally produces arcsecond positions distributed within tens of minutes of the burst.

At the time of this conference, the *Swift* BAT had detected 339 GRBs (at a rate of about 100 per year), of which 88% have XRT followup observations. The XRT had observed 225 GRBs with prompt followup, typically beginning within $\sim$ 100 s after the burst and lasting for days or weeks. The XRT detection rate is 94% for observations of BAT-discovered GRBs for which XRT observations begin within 200 ks of the burst trigger. The detection rate for long GRBs is 97%, while XRT has detected 23 of 31 short GRBs (74%). The UVOT detects optical transients about 40% of the time, with ground-based observations adding another 20%. Roughly 1/3 of *Swift* GRBs have measured redshifts. The current redshift distribution for *Swift* long GRBs is shown in Fig. 2. The median redshift is now 2.0 with a mean of 2.2, down from 2.5 for the first 2 years of the mission (Jakobsson et al. 2006); for reasons we do not understand, no redshifts greater than 4.0 have been measured since GRB 060927. Because of uncertainties in the determination of redshifts for short GRBs, none of which has yet been measured in absorption against the optical transient, and for which host galaxy identification is often problematic, I do not show the distribution of short GRB redshifts, but they
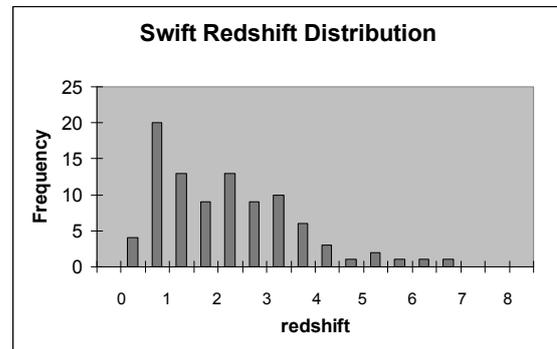

Fig. 2. Redshift distribution of long *Swift* GRBs through June 2008.

tend to be at lower redshifts than long bursts, with a mean redshift of about 0.5 for the best-determined cases.

2. Key *Swift* Discoveries
Here I highlight some of the key discoveries made by *Swift* in its first three years of operation.

2.1. X-ray afterglows
With $\sim$230 prompt X-ray afterglows, the XRT has shown that the early behavior of X-ray afterglows is typically much more complex than the simple power laws observed at later times with *Beppo-SAX* (de Pasquale et al. 2006). X-ray afterglows exhibit a variety of non-power-law behavior in the first several hours, including steep decays generally attributed to the end of the prompt emission, flat plateau segments with very slow decays, and flares (Nousek et al. 2006; Zhang et al. 2006; Panaitescu et al. 2006a). Fig. 3 shows the light curve of GRB 060413, which displays all of these characteristics, and can be considered a prototypical, or "canonical", X-ray light curve. However, we note that X-ray light curves showing all these features are very rare: most X-ray light curves display only some of these phases.

An interesting point that has yet to be settled is the apparent absence of jet breaks at the expected times (Burrows & Racusin 2006; Liang et al. 2008; Racusin et al. 2009, in prep), combined with a related observation of fairly common chromatic behavior between the X-ray and optical bands (Panaitescu et al. 2006b). Some of this behavior may result from insufficient sensitivity to detect very late jet breaks (Curran et al. 2008; Racusin et al. 2009, in prep), while some of it may be due to more complex jet structure than the simple top-hat jet usually assumed (Racusin et al. 2009, in prep; de Pasquale et al. 2008). Further work is needed on this topic.

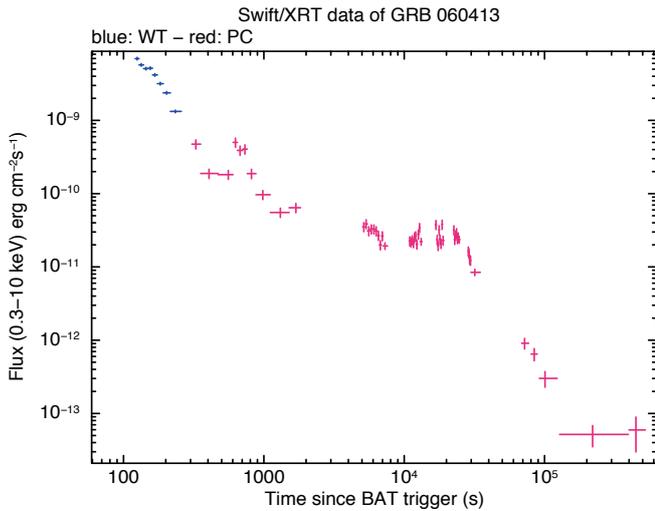Swift/XRT data of GRB 060413

blue: WT – red: PC

Fig. 3. XRT light curve for GRB 060413. Blue data points are in Windowed Timing mode, red data points are in Photon-Counting mode. This light curve shows all the "canonical" features, including a rapid decline, a flare, a plateau phase, and a normal decay phase (though the latter is unusually steep and may actually represent a post-jet break phase in this case).
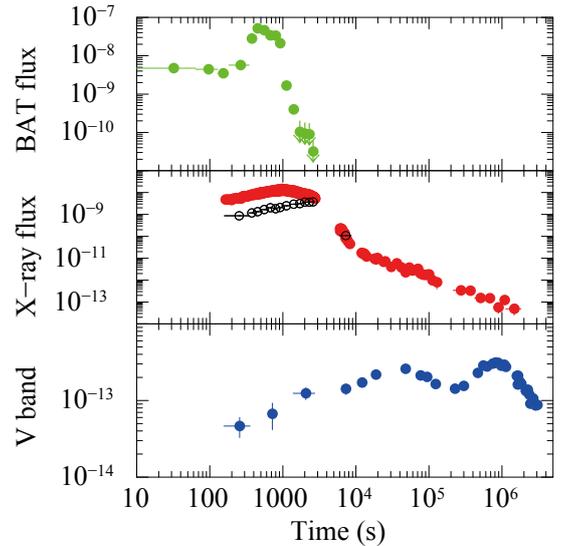
Fig. 4. Top: Swift BAT light curve of GRB 060218. Middle: Swift XRT light curve of GRB 060218. The open circles show the flux due to the black body component. Bottom: Swift UVOT v band light curve of GRB 060218. The first peak is due to the shock breakout, while the second peak is caused by the supernova.

2.2. Short GRB Localizations

One of the most important results from the *Swift* mission has been the localization of short GRBs by the BAT and XRT. At the time of this conference in June 2008, 23 short GRB X-ray afterglows had been localized to precision of several arcseconds. Early results provided dramatic evidence in support of a different origin for short GRBs than for long GRBs, with several cases of short GRB afterglows associated with elliptical galaxies with extremely low rates of star formation (Gehrels et al. 2005; Barthelmy et al. 2005b), in stark contrast to the environment of typical long GRB afterglows (Fruchter et al. 2006). A substantial fraction of the short bursts have been localized to directions with no obvious host galaxy, suggesting that they may have been ejected from their host. Finally, no supernova components have been found associated with short bursts, even when they are at low redshifts. All of these observations are consistent with expectations for compact mergers (NS-NS or NS-BH), which is the favored model for the majority of short GRBs (e.g. Lattimer & Schramm 1976; Paczyński 1986; Eichler et al. 1989; Paczyński 1991).

2.3. GRB 060218: First Detection of Shock Breakout

GRB 060218 was an unusual GRB at a very low redshift. The gamma-ray lightcurve was very smooth and extremely long, with $t_{90} = 2100 \pm 100$ s (Campana et al. 2006). The X-ray light curve was also very long and smooth, peaking at about T+2000 s (Fig. 4). The X-ray spectrum was just as unusual as the light curve: virtually all XRT afterglow spectra can be fit with an absorbed

power law, but this spectrum required an additional soft component consistent with a black body spectrum, suggestive of shock breakout. The radius of the black body component increases in time, and its temperature drops, also consistent with expecteations for shock breakout. However, the radius was found to be significantly larger than expected for a Wolf-Rayet star, the expected progenitor of a GRB. We interpreted the event as a shock breakout from the dense stellar wind surrounding the WR star (Campana et al. 2006; Waxman et al. 2007), the first time that this long-predicted phenomenon has been observed.

3. GRB 080319B: the "Naked-Eye" GRB

19 March 2008 was a busy day for *Swift*, with four GRBs on that day and five GRBs in a 24 hour period! The 2nd of these, GRB 080319B, turned out to be one of the most interesting bursts ever seen (Racusin et al. 2008; Bloom et al. 2008; Kumar & Panaitescu 2008). The optical counterpart peaked at a visual magnitude of 5.3, by far the brightest optical GRB counterpart ever seen (the previous record was grb 990123 at about 9th magnitude). What made this even more remarkable is that the redshift of this GRB is $z = 0.937$ (Vreeswijk et al. 2008). The gamma-ray emission was among the brightest ever observed, and the X-ray afterglow was the brightest seen the the XRT. I refer readers to Racusin et al. (2008) for details of the large set of radio, optical, X-ray and gamma-ray observations our team assembled, together with detailed discussion of the theoretical interpretation
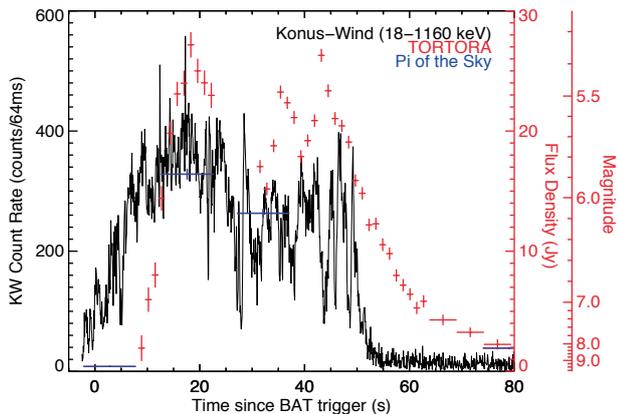
Fig. 5. Prompt light curve of GRB 080319B (Racusin et al. 2008). The black curve shows the Konus-Wind data in the 18 keV - 1.16 MeV energy range. The blue points show the Pi-of-the-Sky optical data, while the red points show the TORTORA optical data. The optical light curves have gaps corresponding to the times when the instruments slewed from GRB 080319A to GRB 080319B. The high resolution TORTORA data peaked at 5.3 magnitudes - by far the brightest optical GRB ever seen!
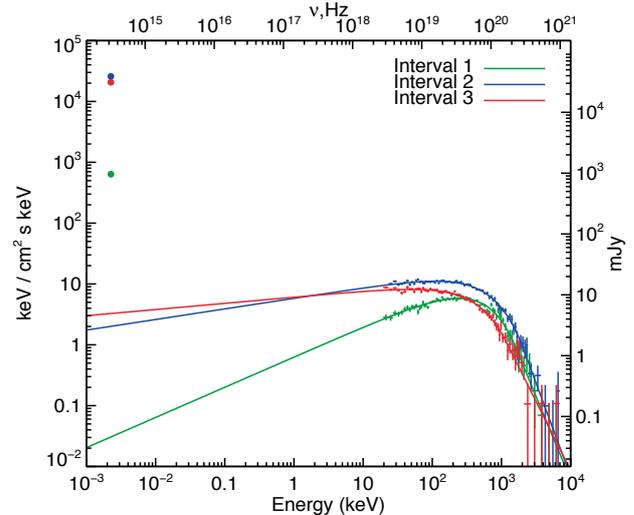

Fig. 6. Spectral Energy Distribution of the prompt emission in three time intervals (Racusin et al. 2008). The data points at about 2 eV represent the Pi-of-the-Sky flux density during these three time intervals. The high energy data points show the Konus-Wind spectrum during these same time intervals, with the curves showing the best-fit Band model extrapolated down to the optical regime. There is strong spectral evolution during the prompt emission, but in all three time intervals the optical flux density exceeds the extrapolation of the gamma-ray flux density by about 4 orders of magnitude, implying that a different spectral component is required to explain the optical flash.

of the data, which I briefly summarize here.

By a fortunate coincidence, GRB 080319B (19B hereafter) occurred only 27 minutes after GRB 080319A, and was located only 10 degrees away on the sky. As a result, 19B was in the field of view of the Pi-of-the-Sky, TORTORA, and RAPTOR optical instruments starting more than 20 minutes before it exploded. The *Swift* slew to 080319A was delayed by nearly 7 minutes due to an Earth limb constraint, but the BAT began collecting event data 1080 s before the burst and registered no precursors in that time period. Fig. 5 shows prompt gamma-ray data from the Konus-Wind instrument, along with prompt optical data from Pi-of-the-Sky and TORTORA.

It is important to note that the first Pi-of-the-Sky data point, which coincides with the BAT trigger, is significantly above the instrumental background and above the earlier data points. The optical flash therefore began within seconds of the gamma-ray burst itself. The optical and gamma-ray emissions clearly occur during the same time interval, though the rapid rise to the optical peak is slightly delayed with respect to the gamma-rays, and the optical decay is slower than the gamma-ray decay. The temporal coincidence of the optical and gamma-ray emission suggests that both bands are produced in the same spatial region. However, the spectrum clearly indicates that different spectral components are required (Fig. 6). A likely interpretation is that the optical emission is synchrotron while the gamma-ray emission is synchrotron self-Compton (Racusin et al. 2008; Kumar &

Panaitescu 2008), in contrast to the usual interpretation of the gamma-ray emission being produced directly by synchrotron. An important prediction of this model is that GeV emission should result from 2nd order Compton scattering; unfortunately, the burst was not visible to the AGILE-GRID instrument and GLAST had not been launched yet, so we have no experimental confirmation of this.

The broad-band afterglow of this burst is shown in Fig. 7. The optical data points exhibit spectral evolution during the first few hours, and deviate strongly from the X-ray afterglow slopes. This strongly chromatic behavior requires a model more complex than a single jet, but can be explained quite well by the two component jet model shown in Fig. 8. In this model, the extremely high bulk Lorentz factor (~ 1000) of the narrow jet is responsible for the extremely bright optical and gamma-ray prompt emission, and the afterglow from this narrow jet dominates the X-ray light curve for the first ~ 12 hours after the burst. The optical afterglow, on the other hand, is dominated in the first hour by the reverse shock of the wide jet, and later by the forward shock of the wide jet. The chromatic behavior is thus explained by our conclusion that the optical and X-ray emission in the first 12 hours are dominated by different jet components. Once the narrow jet breaks, the X-ray emission also becomes
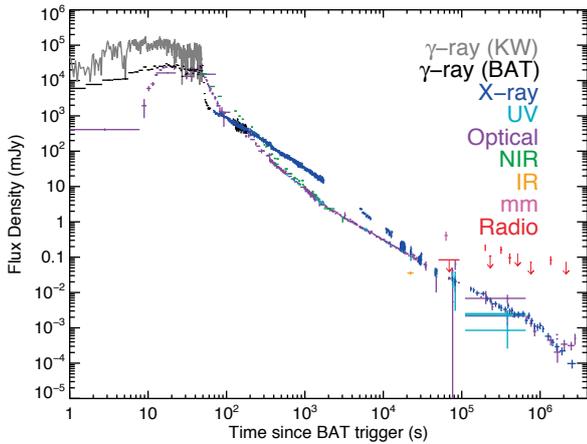
Fig. 7. Broad-band afterglow of GRB 080319B (Racusin et al. 2008). This is a rich data set from a large number of instruments and observing groups; please see Racusin et al. for the complete data list as well as the list of collaborators (co-authors). The prompt emission from *Swift*/BAT (extrapolated into the 0.3-10 keV band for comparison with the XRT data), Konus-Wind, Pi-of-the-Sky, and TORTORA are shown here, together with afterglow emission from *Swift*/XRT, *Swift*/UVOT, a number of ground-based optical telescopes, and several radio telescopes. The optical light curves are normalized to the UVOT v-band data between $T_0 + 1500$ s and $T_0 + 10,000$ s, and show clear evidence for spectral evolution during the first few hours (resulting in apparent discrepancies between different filters around several hundred seconds). The XRT/BAT data are scaled up by a factor of 45 to align the late-time X-ray light curve with the optical light curve, and the Konus-Wind data are scaled up by a factor of 10^4 for comparison with the optical flux densities during the prompt phase.
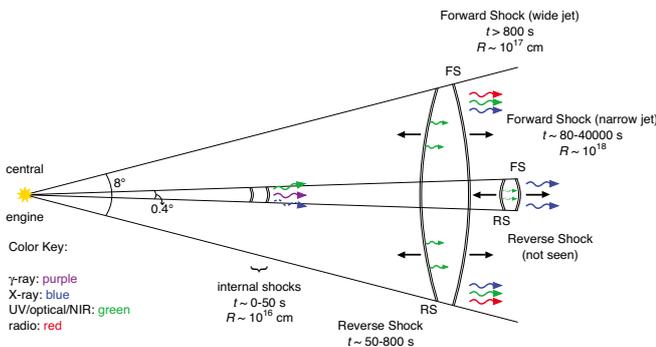

Fig. 8. Schematic diagram of the jet structure of GRB 080319B (Racusin et al. 2008; figure courtesy of J. D. Myers, NASA/GSFC). The chromatic behavior of the optical and X-ray light curves are a result of this complex jet structure. The prompt emission and early X-ray afterglow are dominated by a narrow jet pointed directly at us. The optical emission immediately after the prompt phase is dominated by the reverse shock of a much broader, concentric jet component. This fades rapidly, and by $T_0 + 1000$ s the optical emission is dominated by the wide jet's forward shock. The narrow jet breaks at about half a day, after which the X-ray afterglow is also dominated by the forward shock of the wide jet. Breaks in the X-ray light curve allow the opening angles of both jet components to be measured.

dominated by the forward shock of the wide jet. The two jet breaks seen in the X-ray light curve correspond to jet opening angles of about 0.4 and 8 degrees for the two jets. The energetics of this burst turn out to be comparable to typical GRBs, in spite of the unusual brightness, due to this narrow jet component. We were fortunate to see it - a simple probabilistic argument suggests that such events may be observable roughly once a decade.

4.   The Future of *Swift*

The *Swift* observatory continues to work very well in its fourth year, and the team continues to improve calibration parameters and operating performance. Over the past two years *Swift* has shifted its emphasis from GRBs toward more Target of Opportunity (ToO) observations, and a substantial fraction of our time is now spent on ToOs (see paper by Gehrels in this volume). The success of the mission has been reflected in an extension of its funded operations until at least September 2011. This raises the prospect of exciting collaborative work with several other missions and experiments, in particular:

- GLAST: With the launch of GLAST during this conference, we are just entering the era of GLAST/*Swift* overlap. At the time of this writing, the GLAST Gamma-ray Burst Monitor instrument has already begun detecting bursts in coincidence with *Swift*. We anticipate exciting results stemming from simultaneous *Swift* and GLAST/Large Area Telescope GeV detectors of bursts that may indicate what role second-order Compton process such as that suggested above for GRB 080319B, or other extremely high energy processes, play in black hole formation and GRB explosions.

- LIGO: the gravitational inspiral "chirp" signature of a compact merger event in coincidence with a *Swift* detection of a short GRB would be the "smoking gun" needed to conclusively demonstrate that some fraction of these events originate in binary mergers. The chance of such a coincident detection is improved by the anticipated advent of Enhanced LIGO in 2009, which will double LIGO's detection range for these events. It is conceivable that *Swift* will still be operational when Advanced LIGO goes online, extending sensitivity to compact mergers out to 300 Mpc for NS-NS binaries and out to 650 Mpc for NS-BH binaries, and further improving chances for detection of gravitational wave events coincident with *Swift* bursts.

5.   Beyond *Swift*

GRBs can now be exploited as bright background sources at high redshift in order to study star formation, galaxy
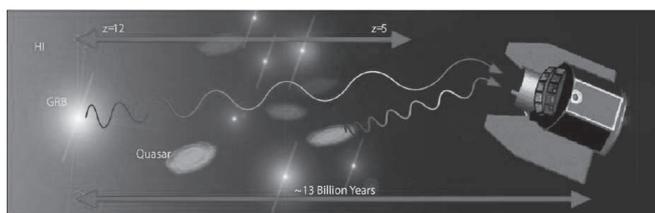
Fig. 9. The *JANUS* mission is designed to study high redshift GRBs and quasars.

evolution, and metal production in the high-z universe (e.g., Prochaska et al. 2007; Tejos et al. 2007; Penprase et al. 2008; Prochaska et al. 2008; Whalen et al. 2008; Fynbo et al. 2008). However, even in the *Swift* era the discovery rate for high-z GRBs is quite low; no burst with $z > 4$ has been found in the past two years, for example. In order to fully exploit this capability, new missions specifically designed to optimize the detection of high redshift bursts *and to measure their redshift directly* are required. One such mission is *JANUS* (Fig. 9), a NASA Small Explorer (SMEX) mission currently in Phase A. *JANUS* carries a wide-field X-ray monitor designed to detect high redshift bursts in the 1-20 keV band, and a Near IR Telecope with a grism designed to measure redshifts between 5 and 12. We expect to detect 25 GRBs per year with redshift greater than 5, providing positions and redshift measurements within 30 minutes of discovery to enable prompt NIR spectroscopy from the ground. *JANUS* will move GRBs beyond the realm of scientific curiosity to the role of an important cosmological tool for studies extending into the reionzation era.

References

Barthelmy, S. D., et al. 2005a, *Space Sci. Rev.*, 120, 143

Barthelmy, S. D., et al. 2005b, *Nature*, 438, 994

Bloom, J. S., et al. 2008, *Ap. J.*, submitted, *arXiv:0803.3215*

Burrows, D. N., et al. 2005, *Space Sci. Rev.*, 120, 165

Burrows, D. N., & Racusin, J. 2006, *Il Nuovo Cimento*, 121, 1273

Campana, S., et al. 2006, *Nature*, 442, 1008

Costa, E., et al. 1997, *Nature*, 387, 783

Curran, P. A., et al. 2008, *MNRAS*, 386, 859

de Pasquale, M., et al. 2006, *Astron. and Astrophys.*, 455, 813

de Pasquale, M., et al. 2008, *AIP Conf. Proc.*, 1000, 463

Djorgovski, S. G., et al. 2008, *Ap. J. (Letters)*, 508, L17

Evans, P. A., et al. 2008, *AIP Conf. Proc.*, 1000, 539

Fruchter, A. S., et al. 2006, *Nature*, 441, 463

Fynbo, J. P. U., et al. 2008, *Ap. J.*, 683, 321

Gehrels, N., et al. 2004, *Ap. J.*, 611, 1005

Gehrels, N., et al., 2005, *Nature*, 437, 851

Goad, M. R., et al. 2007, *Astron. and Astrophys.*, 476, 1401

Jakobsson, P., et al. 2006, *Astron. and Astrophys.*, 447, 897

Klebesadel, R. W., Strong, I. B., and Olson, R. A. 1973, *Ap. J. (Letters)*, 182, L85

Kouveliotou, C., et al. 1993, *Ap. J.*, 413, L101

Kumar, P., & Panaitescu, A. 2008, *MNRAS*, submitted, *arXiv:0805.0144*

Lattimer, J., & Schramm, D. 1976, *Ap. J.*, 210, 549

Meegan, C. A., et al. 1992, *Nature*, 355, 143

Metzger, M. R., et al. 1997, *Nature*, 387, 878

Nousek, J. A., et al. 2006, *Ap. J.*, 642, 389

Mészáros, P., & Rees, M. J. 1993, *Ap. J.*, 405, 278

Paczyński, B. 1986, *Ap. J.*, 308, L43

Paczyński, B. 1991, Acta Astron., 41, 257

Panaitescu, A., et al. 2006a, *MNRAS*, 366, 1357

Panaitescu, A., et al. 2006b, *MNRAS*, 369, 2059

Penprase, B. E., et al. 2008, *AIP Conf. Proc*, 990, 499

Prochaska, J. X., et al. 2007, *Ap. J.*, 666, 267

Prochaska, J. X., et al. 2008, *AIP Conf. Proc*, 1000, 479

Racusin, J. L., et al. 2008, *Nature*, in press, *arXiv:0805.1557*

Rees, M. J., & Mészáros, P. 1992, *MNRAS*, 258, 41P

Roming, P.W.A., et al., 2005, *Space Sci. Rev.*, 120, 95

Tejos, N., et al. 2007; *Ap. J.*, 671, 622

van Paradijs, J., et al. 1997, *Nature*, 386, 686

Vreeswijk, P. M., et al. 2008, *GCN Circ.*, 7444

Waxman, E., Mészáros, P., & Campana, S. 2007, *Ap. J.*, 667, 351

Whalen, D., et al. 2008, *Ap. J.*, 682, 1114

Zhang, B., et al. . 2006, *Ap. J.*, 642, 354